Long-time nonpreaveraged diffusivity and sedimentation velocity of clusters: Applications to micellar solutions

Venkat Ganesan and Howard Brenner
Department of Chemical Engineering, Massachusetts Institute of Technology, Cambridge, Massachusetts 02139-4307
(Received 27 July 1998)

Calculations are presented for the long-time diffusivity and sedimentation velocity of *associating colloids*. Examples of the latter are micellar solutions and microemulsions. The analysis incorporates the role of reversible association-dissociation processes accompanying the physical-space transport of these clusters through the solution. This is accomplished without the need for preaveraging by transforming the association-dissociation processes into equivalent ''size-space'' diffusional processes, which are then embedded into the simultaneous physical-space transport processes occurring in three-dimensional space so as to obtain a four-dimensional convective-diffusion equation governing transport of the clusters in both the physical and size spaces. A generic ''projection'' scheme framework based on generalized Taylor dispersion theory is then applied to the problem, thereby reducing the four-dimensional transport equation to a coarse-grained three-dimensional *physical-space* convective-diffusion equation. Effects arising from the existence of a distribution of cluster sizes are accounted for in the latter formulation governing the *mean* transport process by the appearance of three coarse-grained phenomenological coefficients whose values depend *inter alia* upon the cluster-size distribution. These ''macrotransport'' coefficients include a mean sedimentation velocity vector arising from the action of external forces (if any), a mean molecular diffusivity dyadic, and an additional diffusive-type contribution to the diffusivity corresponding to a convective (''Taylor'') dispersivity. The latter contribution arises as a consequence of the spread in settling velocities of the differently sized clusters. The generic framework developed is illustrated by applications to two classes of micellar solutions: (i) solutions comprised of spherical micelles; (ii) solutions comprised of cylindrical or wormlike micelles (so-called ''living polymers''). Each spherical micelle is modeled as an impenetrable rigid sphere, the radius of which is determined by its aggregation number. The living polymers are modeled by the Debye-Bueche theory, wherein a coiled macromolecular chain is regarded as a Brownian ''spongelike'' porous sphere through whose interior solvent percolates. Calculations of the resulting macrotransport coefficients, including their scaling relationships, are presented for both cases, and their physical significance discussed in terms of the underlying microscale physics. Possible applications and potential extensions of the generic framework are outlined.
[S1063-651X(99)09302-2]

PACS number(s): 82.70.−y, 36.40.Sx, 05.40.−a

I. INTRODUCTION

The present work studies the diffusion and sedimentation of size-fluctuating Brownian ''clusters'' through otherwise quiescent, unbounded fluid continua. These Brownian solutions are assumed to be sufficiently dilute with regard to cluster concentration such that individual clusters do not interact hydrodynamically or physicochemically with one another. Clusters are envisioned as being composed of aggregates of solute molecules, i.e., ''monomers'' (cf. [1] for a general discussion of systems comprising examples of this category). Each cluster is assumed to undergo a reversible association-dissociation (A-D) process, leading to a continuous temporal variation in the number of monomer molecules instantaneously constituting the aggregate. (In the following, the terms ''size'' and ''aggregation number'' are used interchangeably except where a need arises to distinguish between them.) A situation of dynamical equilibrium as regards the cluster-size distribution is ultimately expected to arise locally at each point of the fluid as a consequence of the inherently reversible nature of these A-D processes coupled with the relative rapidity of their kinetics compared with physical-space cluster transport rates. Because of this, it suffices to focus attention on the transport of a single representative cluster, hereafter termed a ''tracer.'' The focus of our analysis is to quantify during such a scenario the transport of such a tracer cluster through the fluid continuum. The cluster is assumed to undergo both physical-space diffusion (due to thermal fluctuations) and sedimentation (due to external forces, if any), simultaneously accompanied by a continuous variation in its size due to the A-D processes. Of course, sedimentation will be absent in the case of force-free solute molecules, in which circumstances only molecular diffusion of the cluster occurs.

The feature of this problem that, to our knowledge, has not previously been addressed in a systematic and rigorous manner is the effect of the short-time cluster-size variation (due to the A-D processes) on the long-time physical-space transport processes. This temporal variation in cluster size manifests itself via an instantaneous size-specific translational diffusion coefficient and sedimentation velocity, each of which varies continuously during the movement of the cluster through the solution owing to changes in its size arising from the A-D processes. This temporal variation in size has a nontrivial effect on the physical-space transport properties of such dispersions. Most prior studies of cluster transport processes have been limited to evaluating the cluster

mobility for the *preaveraged* case, where the cluster size is assumed to remain fixed at its equilibrium mean value during its entire motion through the solvent (see, for example, [2]). In contrast, we treat here the nonpreaveraged case, where the cluster is allowed to undergo relatively rapid fluctuations in its size due to the A-D processes as it wends its way through the solution.

Practical motivations for studying cluster transport processes are manifold. Association colloids are ubiquitous in nature, micellar dispersions and microemulsions [3,4] representing common examples. Equilibrium aspects of these solutions have been widely studied, including elucidating the many size and shape distributions thermodynamically possible in such systems. In contrast, the transport or nonequilibrium properties of these entities have received only sparse attention. In this context it is pertinent to note the emergence of recent interest in quantifying the rheology of clustering systems, exemplifying the more general class of so-called soft glassy systems [5,6]. The same features that lead to intriguing thermodynamics [3] (namely, equilibrium size and shape distribution features) make the analysis of transport properties equally interesting, albeit more complex. In this initial foray into the field we do not address larger issues relating to the rheology of these systems when they undergo shear. Rather, we study only those more limited features accompanying the transport of clusters through otherwise quiescent systems in which shear is absent.

Owing to the polydispersivity of cluster sizes, transport processes occurring in these systems exhibit interesting attributes not present in monodisperse systems. Explicitly, we will quantify both the diffusivity and sedimentation (i.e., mobility) coefficient in dilute clustering systems. The diffusion coefficient is shown to involve an additional contribution (termed the ''convective'' or ''Taylor'' dispersivity) above and beyond the ordinary molecular contribution, which arises from the distribution of settling velocities among the differently sized clusters. Furthermore, our analysis indicates that the size-fluctuation processes accompanying the *microscale* physical-space cluster transport processes may have a significant effect upon the *macroscale* physical-space transport coefficients. On the practical side we note that self-diffusion coefficients are widely used to characterize such features as size, shape, and cluster-cluster interactions in these systems [7–9]. As such, our analysis points up a scheme whereby key phenomena arising in these polydisperse systems can be accounted for when interpreting experimental self-diffusion and electrophoretic measurements in such clustering systems.

A modest prior literature examines several elements closely related to our study. Notably, Cussler [10] considered cluster diffusion in solutions near the consolute point, where very large sizes of the diffusing units (''clusters'')—certainly bigger than the underlying monomeric molecular units—are to be expected. Frankel, Mancini, and Brenner [11] investigated a system similar in spirit to ours, relating to diffusion and sedimentation coefficients in solutions of coiled linear polymer molecules, and arising from Brownian size fluctuations stemming from the inherently flexible nature of such entities. Our goal here is the development of a generic conceptual framework for quantifying the transport of dispersions of association colloids, with the accompanying association-dissociation process viewed as diffusional processes in ''size'' or ''aggregation number'' space (cf. also Ziabicki [12]). Other continuum approaches have been proposed for quantifying the cluster-size distributions—see, e.g., [13]. Our analysis draws heavily upon generalized Taylor dispersion theory [14].

The scheme ultimately developed will be illustrated by applications to two distinct, but interrelated examples of micellar cluster geometries. The first involves a micellar solution composed of spherical micelles, for which the size distribution encountered in practice is typically confined to a relatively narrow range centered about the mean aggregation number [4]. In the second case we consider similar phenomena for cylindrical micelles, frequently termed ''living polymers.'' The latter exhibit a wide range of cluster sizes, ranging from monomeric to polymeric, the latter involving very large aggregation numbers. Pioneering studies of these systems appear in the works of Cates [15,16], Bouchaud [17,18], and others, who investigated the dynamics of these systems in the entangled-regime domain. Our analysis will focus on the diffusive and sedimentary aspects of these systems, albeit in the dilute regime.

In the dilute cluster solution limit it suffices to focus attention on the transport of a single cluster. In the subsequent analysis, hydrodynamic as well as physicochemical intercluster interactions are neglected, permitting attention to be focused exclusively on the effect of the internal A-D processes. Furthermore, owing to the dilute nature of the dispersion, only pairwise A-D reactions need to be considered. These assumptions, which hold in the dilute solution limit, ensure that the effective transport properties of the solution can be discerned by employing a tracer cluster to sample the configurational space (size- plus physical-space coordinates) of the clusters present in the solution. An exact microscale description of the transport process would require calculating the multivariate probability density function $P(\mathbf{R},n,t)$ of the tracer cluster, defined in the four-dimensional configurational space described at time t by the three scalar physical coordinates parametrizing the instantaneous position vector $\mathbf{R}$ (of say, the center of mass) of the cluster in physical space, and the cluster aggregation number n. In most cases, however, physical interest does not center on the detailed microscale description provided by $P(\mathbf{R},n,t)$ but rather on a coarse-grained macroscale probability density $\overline{P}(\mathbf{R},t)$ characterizing the totality of the molecular solute species being transported, irrespective of the size of the cluster in which the monomer molecule characterizing the chemical species being transported finds itself at any given instant of time. The less detailed density distribution $\overline{P}(\mathbf{R},t)$ quantifies the solute species transport process through three-dimensional physical space (i.e., through the solution), accounting for variations occurring in cluster size in an appropriately averaged manner that eschews preaveraging.

This coarse-grained density is expected to evolve asymptotically according to the macroscale, i.e., physical-space convective-diffusive conservation equation [14]

$$\frac{\partial \overline{P}}{\partial t} + \overline{\mathbf{U}} \cdot \boldsymbol{\nabla} \overline{P} = \overline{\mathbf{D}} : \nabla \nabla \overline{P}, \tag{1}$$

wherein the time- and position-independent sedimentation

vector velocity $\overline{\mathbf{U}}$ and dispersion dyadic $\overline{\mathbf{D}}$, respectively, quantify the coarse-grained convective and diffusive solute transport mechanisms in the fluid continuum. Implicitly embedded within these coefficients are the overall effects of the comparable microscale transport processes arising from the continuous variations in cluster size. For a monodisperse system (of aggregation number $\overline{n}$) these coefficients are, respectively, identical to the Stokes settling velocity $\mathbf{U}\equiv\mathbf{U}(\overline{n})$ and molecular diffusivity $\mathbf{D}\equiv\mathbf{D}(\overline{n})$ appropriate to clusters of size $\overline{n}$. Our objective is, starting from the specified microscale transport data, to calculate the coefficients $\overline{\mathbf{U}}$ and $\overline{\mathbf{D}}$ governing the macroscale transport processes for circumstances where a distribution of cluster sizes exists owing to the A-D processes.

II. FORMULATION

As indicated in the Introduction, attention is directed towards the transport of a single cluster undergoing fluctuations in size due to the reversible A-D processes. Conformational changes in *shape*, though potentially interesting, are not considered in this work. A variety of schemes can be imagined for the A-D processes accompanying the physical-space transport. However, many such processes lead to reaction schemes that can be represented physically as size-space diffusional processes, with an internal force-derived potential energy function restricting the cluster size range. Our analysis will, in general, focus only upon those reaction schemes for which such a *diffusion equation* representation is consistent with the underlying physics [12].

The starting point for our analysis is the four-dimensional microscale conservation equation governing both size-specific spatial ($\mathbf{R}$) and position-specific aggregational (n) transport of the tracer cluster through the unbounded fluid:

$$\frac{\partial P}{\partial t}+\boldsymbol{\nabla}\cdot\mathbf{J}=j_n-j_{n-1}, \tag{2}$$

where $P\equiv P(\mathbf{R},n,t|\mathbf{R}',n_0)\equiv P(\mathbf{R}-\mathbf{R}',n,t|n_0)$ represents the complete microscale conditional probability density (Green's function) signifying the probability that at a time t the tracer cluster is of aggregation number n and is located at position $\mathbf{R}$, given that at time $t=0$ the cluster was centered at position $\mathbf{R}'$ and was of size n_0 [19]. The operator $\nabla\equiv(\partial/\partial\mathbf{R})_{n,t}$ denotes the size-specific physical-space gradient operator. The physical- and size-space fluxes of the probability density P, are denoted respectively by $\mathbf{J}$ and j. In situations wherein a large range of aggregation numbers are possible (such as will be assumed of all the examples considered in this paper), it is permissible to replace the above discrete ''diffusion equation'' (2) by a version involving a continuously varying index n:

$$\frac{\partial P}{\partial t}+\boldsymbol{\nabla}\cdot\mathbf{J}+\frac{\partial j}{\partial n}=0, \tag{3}$$

wherein $j\equiv j(\mathbf{R},n,t|n_0)$ now represents the size-space flux, a continuous function of n, and $\partial/\partial n\equiv(\partial/\partial n)_{\mathbf{R},t}$ denotes the position-specific size-space gradient operator.

The fluxes $\mathbf{J}$ and j, can be expected constitutively [14] to possess conventional convective and diffusive contributions as follows:

$$\mathbf{J}=M(n)\mathbf{F}(n)P-D(n)\nabla P, \tag{4}$$

$$j=m(n)f(n)P-d(n)\frac{\partial P}{\partial n}, \tag{5}$$

wherein $M(n)$ denotes the physical-space cluster mobility coefficient, and $\mathbf{F}(n)$ the external vector force exerted on the cluster as a whole. Their respective counterparts in size space are denoted by $m(n)$ and $f(n)$. Diffusivities in physical and size space, respectively, denoted by $D(n)$ and $d(n)$, are related to the respective hydrodynamic mobility coefficients through configuration-specific Stokes-Einstein relations [20]:

$$D(n)=k_BTM(n),\quad d(n)=k_BTm(n), \tag{6}$$

with k_B the Boltzmann constant. For the reversible reaction schemes subsequently considered, the scalar force $f(n)$ can always be written as the negative size-space gradient of a potential energy function $V(n)$ (see Appendices A and B). Use of this information together with Eq. (6) permits Eq. (5) to be rewritten as

$$j=-d(n)\exp[-V(n)/k_BT]\frac{\partial}{\partial n}\{P\exp[V(n)/k_BT)]\}. \tag{7}$$

The above microscale data are to be supplemented by respective physical- and size-space boundary conditions. The former is embodied in the generic requirement that all the algebraic moments of the distribution function P converge, namely, [21]

$$|\mathbf{R}-\mathbf{R}'|^mP\to 0\quad (m=0,1,2,\ldots)\ \text{ as }\ |\mathbf{R}-\mathbf{R}'|\to\infty, \tag{8}$$

and the latter as

$$j=0\ \text{ for }\ n=1,\infty. \tag{9}$$

In addition, we have for the initial condition that

$$P=\begin{cases}\delta(\mathbf{R}-\mathbf{R}')\,\delta(n-n_0) & (t=0),\\ 0 & (t<0),\end{cases} \tag{10}$$

with δ the Dirac δ function, and n_0 the initial size of the cluster at time $t=0$. Satisfaction of Eq. (8) assures the convergence of the various momental integrals arising in the general theory [14]. It is also readily verified from the above system of equations that the solution P satisfies the normalization condition

$$\int_{\mathbf{R}_\infty}\int_1^\infty P(\mathbf{R}-\mathbf{R}',n,t|n_0)\,dn\,d^3\mathbf{R}=1\quad (t>0)\quad \forall(n_0,\mathbf{R}'). \tag{11}$$

In the above, $d^3\mathbf{R}$ denotes a volume element in three-dimensional physical space and dn the comparable-size space incremental element. Size space is assumed to extend from the basic monomer unit ($n=1$) to clusters of size $n=\infty$. Note that we have used the Euler-Maclaurin sum for-

mula to replace the sum over the discrete index n by a comparable integration over the continuous index n. Equation (11) shows that the total probability of finding the tracer somewhere in physical space, $\mathbf{R}_\infty:\{-\infty<x_i<\infty;\ i=1,2,3\}$, and contained within a cluster of some size $n:\{1\leqslant n<\infty\}$ is conserved at each instant.

As stated in the Introduction, physical interest generally centers not on the four-dimensional microscale distribution P, but rather only on the coarse-scale macroscopic descriptor $\overline{P}$ of the transport processes occurring in three-dimensional physical space, as embodied in the macroscale conditional density:

$$\overline{P}(\mathbf{R}-\mathbf{R}',t|n_0)\overset{\text{def.}}{=}\int_1^\infty P(\mathbf{R}-\mathbf{R}',n,t|n_0)\,dn. \tag{12}$$

It is an immediate consequence of Eqs. (11) and (12) that this coarse-grained probability is conserved in physical space:

$$\int_{\mathbf{R}_\infty}\overline{P}(\mathbf{R}-\mathbf{R}',t|n_0)\,d^3\mathbf{R}=1 \quad (t>0) \quad \forall(n_0,\mathbf{R}'). \tag{13}$$

Asymptotically, for sufficiently long times (see below), $\overline{P}$ is independent of the initial cluster size n_0 [14], and hence is functionally of the form $\overline{P}(\mathbf{R}-\mathbf{R}',t)$.

The initial- and boundary-value problem posed by the system of microscale equations (3)–(11) possesses the same physicomathematical structure as that of the generic problem of generalized Taylor dispersion theory [14]. This equivalence is established when one identifies the size (n) and physical-space position ($\mathbf{R}$) with the respective ''local'' ($\mathbf{q}$) and ''global'' ($\mathbf{Q}$) coordinates of the latter theory. Generalized Taylor dispersion theory shows that, for long times, namely, $\|d(n)\|t/\overline{n}^2\gg 1$ (with $\|d(n)\|$ denoting some norm of the size-space diffusivity, and $\overline{n}$ denoting the mean aggregation number), the asymptotic solution P of Eq. (3) satisfying Eqs. (4)–(11) matches momentwise the comparable dominant long-time asymptotic solution of $\overline{P}$, whose transport through physical space is governed by Eq. (1) together with the respective boundary and initial conditions

$$|\mathbf{R}-\mathbf{R}'|^m\overline{P}\to 0 \quad (m=0,1,2,\ldots) \ \text{ as } \ |\mathbf{R}-\mathbf{R}'|\to\infty \tag{14}$$

and

$$\overline{P}=\begin{cases}\delta(\mathbf{R}-\mathbf{R}') & (t=0),\\ 0 & (t<0).\end{cases} \tag{15}$$

Furthermore, by virtue of having matched the respective moments of $\overline{P}$ and P, the theory also provides an explicit scheme for determining the macrotransport coefficients $\overline{\mathbf{U}}$ and $\overline{\mathbf{D}}$ via appropriate quadratures of the specified microscale phenomenological data [data explicitly embodied in the microscale transport coefficients, and implicitly appearing in Eqs. (3)–(5)] over the cluster-size domain.

Implementation of the theory [14] requires, *inter alia*, knowledge of the solution of a steady-state scalar field $P_0^\infty(n)$, the latter corresponding to the steady, long-time limit of the unsteady-state conditional probability density,

$$P_0(n,t|n_0)\overset{\text{def.}}{=}\int_{\mathbf{R}_\infty}P(\mathbf{R}-\mathbf{R}',n,t|n_0)\,d^3\mathbf{R},$$

that the cluster possesses a size n at time t irrespective of its physical-space location $\mathbf{R}$. The field $P_0^\infty(n)$ satisfies the steady-state differential equation

$$\frac{dj_0^\infty}{dn}=0, \tag{16}$$

with

$$j_0^\infty(n)\overset{\text{def.}}{=}-d\exp(-V/k_BT)\frac{d}{dn}[P_0^\infty\exp(V/k_BT)], \tag{17}$$

in which the latter flux density satisfies the boundary conditions

$$j_0^\infty=0 \quad \text{at } \ n=1,\infty \tag{18}$$

together with the normalization condition

$$\int_1^\infty P_0^\infty\,dn=1. \tag{19}$$

The solution of Eqs. (16)–(19) is

$$P_0^\infty(n)=\left\{\int_1^\infty\exp[-V(n)/k_BT]dn\right\}^{-1}\exp[-V(n)/k_BT]. \tag{20}$$

The macrotransport coefficients $\overline{\mathbf{U}}$ and $\overline{\mathbf{D}}$ appearing in Eq. (1) are expressed in terms of respective quadratures of $P_0^\infty(n)$ [14]. In this manner the average settling velocity $\overline{\mathbf{U}}$ of the cluster is given by

$$\overline{\mathbf{U}}=\overline{U}\hat{\mathbf{F}}, \tag{21}$$

where

$$\overline{U}\equiv\langle U(n)\rangle\overset{\text{def.}}{=}\int_1^\infty dn\,P_0^\infty(n)U(n), \tag{22}$$

in which

$$U(n)=M(n)F(n) \tag{23}$$

is the settling velocity of an aggregate of size n, and $\hat{\mathbf{F}}=\mathbf{F}/F(n)$ represents a unit vector in the spatial direction parallel to the applied force $\mathbf{F}$, in which $F(n)=|\mathbf{F}(n)|$.

The dispersivity dyadic is represented by the sum [14]

$$\overline{\mathbf{D}}=\overline{D}^M\mathbf{I}+\overline{D}^C\hat{\mathbf{F}}\hat{\mathbf{F}}, \tag{24}$$

wherein

$$\overline{D}^M \equiv \langle D^M(n)\rangle \overset{\text{def.}}{=} \int_1^\infty dn\, P_0^\infty(n) D(n)$$

$$\equiv k_B T \int_1^\infty dn\, P_0^\infty(n) M(n) \tag{25}$$

is the average physical-space molecular diffusivity of the cluster, and

$$\overline{D}^C = \int_1^\infty dn\, P_0^\infty(n) B(n)[U(n) - \overline{U}] \tag{26}$$

represents the Taylor or convective contribution to the dispersivity. The latter contribution stems from the continuous variation in settling velocity arising from the size-space transport processes (i.e., due to continuous changes in the size of the cluster as it traverses the fluid).

Appearing in the latter integral is yet another time-independent scalar field, $B(n)$, which represents the solution of the differential equation (14)

$$j_0^\infty(n) \frac{dB}{dn} - \frac{d}{dn}\left[P_0^\infty d(n) \frac{dB}{dn}\right] = P_0^\infty(n)[U(n) - \overline{U}], \tag{27}$$

subject to the boundary conditions

$$\frac{dB}{dn} = 0 \quad \text{at} \quad n = 1, \infty. \tag{28}$$

The solution of Eqs. (27) and (28) can easily be obtained from the knowledge of the field P_0^∞ given by Eq. (20), yielding

$$B(n) = b_0 - \int_1^n dn' \frac{\exp[V(n')/k_B T]}{d(n')} \times \int_1^{n'} d\tilde{n}[U(\tilde{n}) - \overline{U}] \exp[-V(\tilde{n})/k_B T], \tag{29}$$

where b_0 is an integration constant whose numerical value is irrelevant in establishing $\overline{D}^C$ via Eq. (26). Substitution of Eq. (29) into Eq. (26) yields the following expression for $\overline{D}^C$:

$$\overline{D}^C = \left\{ \int_1^\infty dn \exp[-V(n)/k_B T]\right\}^{-1} \times \int_1^\infty dn'' \frac{\exp[V(n'')/k_B T]}{d(n'')} \times \left\{ \int_1^{n''} dn'[U(n') - \overline{U}] \exp[-V(n')/k_B T]\right\}^2. \tag{30}$$

Explicit calculation of $\overline{U}$, $\overline{D}^M$, and $\overline{D}^C$ from the preceding formulas requires specifying constitutive equations for both the size- and physical-space mobility coefficients, $m(n)$ and $M(n)$, respectively, as well as the size-space potential $V(n)$. As already indicated, a variety of schemes can be imagined for constitutively quantifying the A-D size-space transport processes. However, the above formulation is sufficiently general to provide robust generic prescriptions for determining the three macrotransport coefficients pending explicit specification of the requisite constitutive relationships.

An outline of the rest of the paper is as follows: To place the preceding concepts on a firmer basis while also illustrating the significance of size variation effects, two distinct A-D schemes will be considered. Appendices A and B each outline respective schemes whereby the master equation for the size-space transport processes can be recast into a diffusion equation format, thereby identifying both $d(n)$ and $V(n)$. Subsequently, in Secs. III and IV we revert to the generic quadrature formula developed in Sec. II, using appropriate models for the physical-space transport coefficients $M(n)$ [and hence $D(n)$] to obtain the macrotransport coefficients $\overline{\mathbf{U}}$ and $\overline{\mathbf{D}}$. Section V concludes with an outlook for future research directions.

III. MACROTRANSPORT COEFFICIENTS FOR SPHERICAL MICELLAR SOLUTIONS

Identification of the size-space mobility coefficient $m(n)$ and the potential energy driving force $V(n)$ for the spherical micelle case is effected in Appendix A. The latter identifies the potential in terms of the mean aggregation number $\overline{n}$ and spread σ in the chemical potential distribution. Calculation of the macrotransport coefficients requires specification of the physical-space mobility coefficient $M(n)$ and force $F(n)$. For the present spherical micellar case the physical-space mobility coefficient can be obtained from Stokes law by modeling the cluster as an impermeable sphere of radius r. The corresponding mobility then scales inversely with the radius of the sphere. The radius of the spherical micelle can itself be related to the aggregation number as

$$r(n) \propto n^{1/3}, \tag{31}$$

whence the mobility obeys the relationship

$$\frac{M(n)}{M(\overline{n})} = \frac{n^{-1/3}}{\overline{n}^{-1/3}}. \tag{32}$$

Furthermore, using the fact that the force $F(n)$ on a cluster scales with n, we have that

$$\frac{U(n)}{U(\overline{n})} = \frac{n^{2/3}}{\overline{n}^{2/3}}. \tag{33}$$

This serves to identify the physical-space coefficients prerequisite to calculating the macrotransport coefficients $\overline{\mathbf{U}}, \overline{\mathbf{D}}$ via Eqs. (21)–(25) and Eq. (30). The remaining size-space coefficients are identified in Appendix A [cf. Eqs. (A14) and (A15)].

Use of the preceding identifications in Eq. (20) yields

$$P_0^\infty(n) = \left\{ \int_1^\infty dn \exp\left[-\frac{(n-\overline{n})^2}{2\sigma^2}\right]\right\}^{-1} \exp\left[-\frac{(n-\overline{n})^2}{2\sigma^2}\right]. \tag{34}$$

The fact that the lower limit of integration in the normalizing weight function is cut off at $n=1$ rather than $n=0$ results in analytic expressions that are quite cumbersome. However, the computed values do not depend crucially on the lower limit used in evaluating the above integrals so long as the mean aggregation number is sufficiently large and the distributional spread small compared with the mean aggregation number. This represents the situation typically encountered for spherical micellar solutions [4]. In such circumstances it is possible to replace the lower integration limit by $n=0$ without significant error. The resulting expressions for the macrotransport coefficients obtained from Eqs. (21)–(25) and Eq. (30) can then be generically expressed in terms of a scaling function as

$$\psi=\overline{n}^{\nu}f(\tilde{\sigma}), \tag{35}$$

wherein ψ represents a generic macrotransport coefficient and f denotes a scaling function that exhibits the following behavior:

$$f(x)\rightarrow\begin{cases}1 & (x\rightarrow 0),\\ x^{\alpha} & (x\gg 1),\end{cases}$$

in which the exponents α and ν [22] depend upon the specific transport coefficient being considered. Also appearing in Eq. (35) is the weighted distributional spread:

$$\tilde{\sigma}\overset{\text{def.}}{=}\frac{\sigma}{\overline{n}^{1/2}}. \tag{36}$$

When the lower limit in Eq. (34) cannot be replaced by zero, such as occurs when the spread satisfies the inequality $\tilde{\sigma}>1$, the above scaling arguments do not hold and the resulting transport coefficients depend nontrivially on the mean aggregation number $\overline{n}$. Despite the fact that some of the assumptions underlying the analysis do not remain rigorously valid in such circumstances [cf. the discussion preceding Eq. (A15)] we have nevertheless also studied such cases.

The analytic quadratures obtained by substituting Eqs. (32)–(34) into Eqs. (21)–(25) for the $n=0$ case can be expressed in terms of parabolic cylinder functions, whose asymptotic expansions are well documented [23]. In the following discussion, however, owing to their algebraic complexity we do not present explicit analytic expressions for the resulting macrotransport coefficients, as such formulas are not very illuminating in and of themselves. Instead, we indicate qualitative features (obtained numerically) describing the functional dependence of the macrotransport coefficients upon the spread in cluster sizes. All of the resulting features are graphically indicated in terms of the scaling variable $\tilde{\sigma}$. Even in those cases wherein replacement of the lower integration limit by zero does not strictly hold, we found that the qualitative features displayed in the subsequent plots are not significantly altered. Accordingly, we have restricted ourselves in what follows primarily to studying the effect of the scaled variable $\tilde{\sigma}$ upon the three macrotransport coefficients.

Mean velocity of settling. Figure 1 depicts the effect of the size-distribution spread upon the ratio of the mean cluster settling velocity $\overline{U}$ to that of the settling velocity $U(\overline{n})\equiv M(\overline{n})F(\overline{n})$ at the mean aggregation number. Initially, for small departures from monodispersivity, this ratio decreases below unity, followed by a steep rise thereafter. The physical explanation of this behavior is straightforward: As already noted, the settling velocity scales as $n^{2/3}$. For small values of the spread $\tilde{\sigma}$, the smaller values of n are sampled more frequently than are the larger values (cf. [24] for a simple proof). This leads to a reduction in the mean settling velocity below that which would have occurred had the tracer size simply coincided with the mean aggregation number. However, at the larger values of $\tilde{\sigma}$ the lower limit is cut off at $n=1$, whereas no such constraint exists for the upper limit. Thus, when the chemical potentials are such that a large spread in the distribution occurs, the mean settling velocity will generally far exceed the settling velocity occurring at the mean aggregation number. Furthermore, from the computed values it can be discerned that the scaling function in the above exhibits exponents $\nu=\frac{1}{3}$ and $\alpha\sim\frac{2}{3}$ (cf. [25] for a simple proof of the value of the latter exponent α).

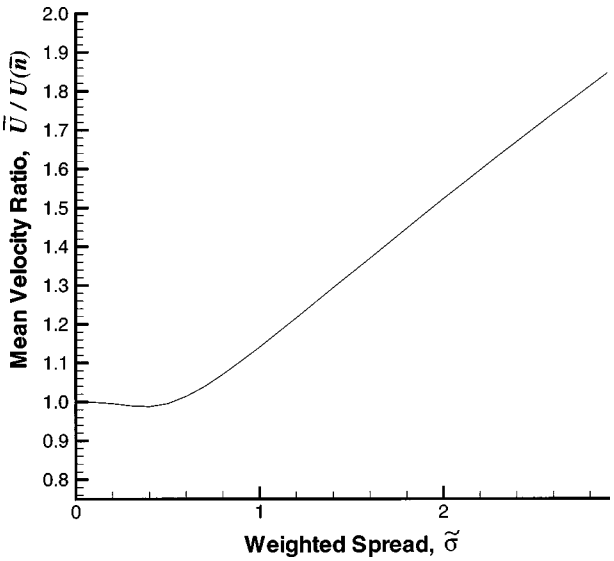

FIG. 1. Effect of polydispersivity $\tilde{\sigma}$ on the mean settling velocity ratio $\overline{U}/U(\overline{n})$ for spherical micellar solutions.

Mean diffusivity. Polydispersivity effects on the normalized mean molecular diffusivity, $\overline{D^M}/D^M(\overline{n})$ are portrayed in Fig. 2. Since the microscale diffusivity $D(n)$ scales as $n^{-1/3}$ the observed variation is consistent with the expected initial rise deriving from the preferential sampling of the smaller aggregation numbers, followed by a manifestation of the effect of the cut off at the lower aggregation number limit. Scaling exponents for this case were determined from the plots to be $\nu=-\frac{1}{3}$ and $\alpha=-0.4$.

Convective dispersivity. Figure 3 depicts the effect of varying the size distribution on the convective dispersivity, indicating a monotonic increase with increasing departure from monodispersivity. No counterpart of this Taylor dispersion phenomenon arises during either the diffusion or sedimentation of *monodisperse* clusters. The qualitative trends depicted in Fig. 3 are completely consistent with the fluctuational origins of $\overline{D^C}$.

Significance of results. The above plots display the respective variations in the three macrotransport coefficients caused by the size-induced spread in chemical potential. Each manifests polydispersivity effects resulting from the

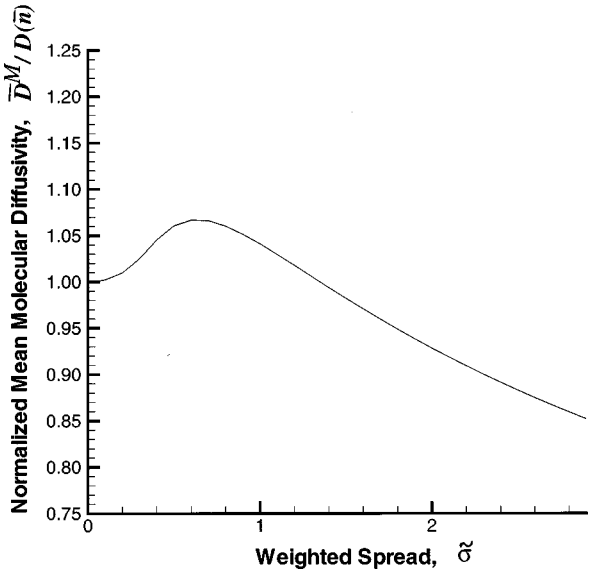

FIG. 2. Effect of the polydispersity $\tilde{\sigma}$ on the normalized mean molecular diffusivity $\overline{D}^M/D(\overline{n})$ for spherical micellar solutions.

reversible A-D processes, wherein the cluster-size growth mechanism occurs by stepwise association processes. In practical situations involving spherical micellar solutions the above effects are unlikely to prove very significant owing to the relatively low polydispersivity indices typically encountered in such systems. Nevertheless, our analysis provides rigorous estimates of the magnitudes of such effects. A perhaps unexpected feature of this example is the existence of a convective or Taylor contribution to the diffusional process, a phenomenon that has no counterpart in monodisperse micellar solutions.

It might appear that the above features with respect to both the mean molecular diffusivity and mean settling velocity could be subsumed under the choice of an appropriately defined mean aggregation number. For instance, one might

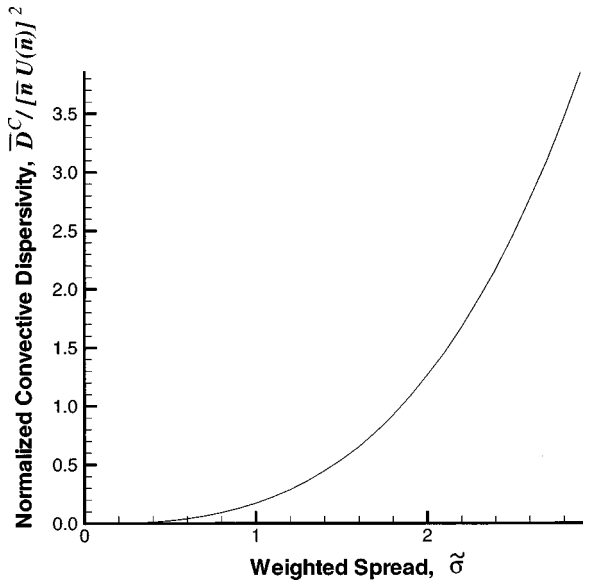

FIG. 3. Dependence of the normalized convective dispersivity $\overline{D}^C/[\overline{n}U(\overline{n})]^2$ on the degree of polydispersivity $\tilde{\sigma}$ for spherical micellar solutions.

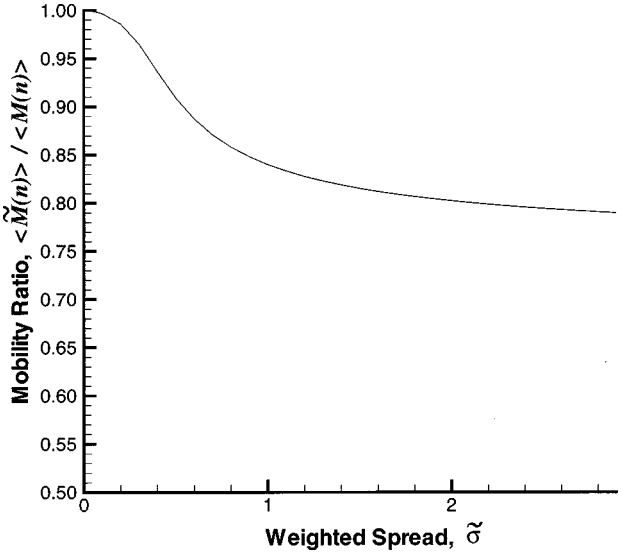

FIG. 4. Dependence of the mobility ratio $\langle\tilde{M}(n)\rangle/\langle M(n)\rangle$ on the polydispersity parameter $\tilde{\sigma}$ for spherical micellar solutions.

propose to define a mean aggregation number, $\tilde{n}$, say, based upon the observed settling velocity:

$$\frac{\overline{U}}{U(\overline{n})}=\frac{\tilde{n}^{2/3}}{\overline{n}^{2/3}}. \tag{37}$$

This choice would, however, imply that

$$\frac{\overline{D}^M}{D(\overline{n})}\neq\frac{\tilde{n}^{-1/3}}{\overline{n}^{-1/3}}, \tag{38}$$

an apparent violation of the Stokes-Einstein equation owing to the fact that

$$\overline{U}=\langle M(n)F(n)\rangle\neq\langle M(n)\rangle\langle F(n)\rangle. \tag{39}$$

If, alternatively, one chose to define a mean mobility coefficient such that

$$\langle\tilde{M}(n)\rangle\overset{\text{def.}}{=}\frac{\overline{U}}{\langle F(n)\rangle}, \tag{40}$$

then

$$\overline{D}^M=k_BT\langle M(n)\rangle\neq k_BT\langle\tilde{M}(n)\rangle. \tag{41}$$

The latter serves to quantify the apparent violation of the Stokes-Einstein relationship. Figure 4 displays the ratio $\langle\tilde{M}(n)\rangle/\langle M(n)\rangle$ obtained for different $\tilde{\sigma}$.

Illustrated in this section were several effects arising from the spread in cluster sizes about a mean aggregation number. Specifically, the spherical micellar solution case was motivated by the availability of the constitutive equations for the microscale size- and physical-space transport coefficients. The next section quantifies similar behavior for another important case, wherein the cluster size distribution exhibits novel features not present in the spherical micellar case.

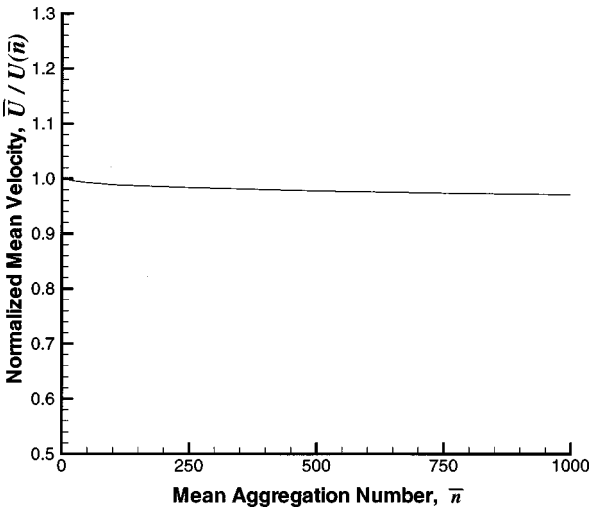

FIG. 5. Effect of the mean aggregation number $\overline{n}$ on the mean velocity ratio $\overline{U}/U(\overline{n})$ for wormlike micellar solutions.

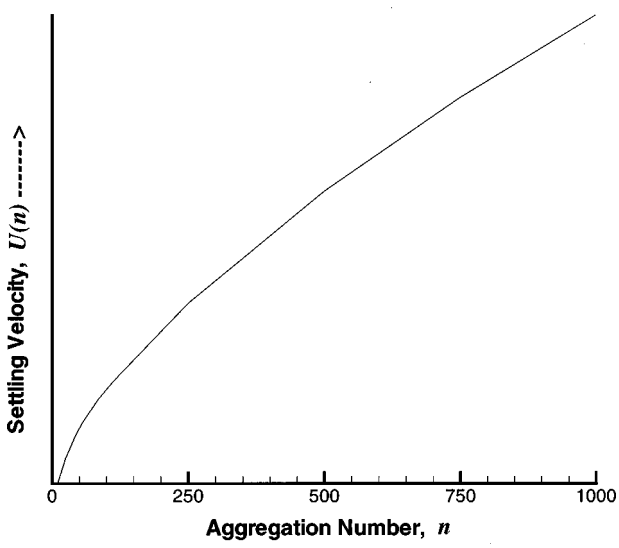

FIG. 6. Variation of the settling velocity $U(n)$ with cluster size n for monodisperse wormlike micellar solutions. Since only the qualitative features of this behavior are of interest we do not explicitly display values for $U(n)$ (a dimensional quantity).

IV. MACROTRANSPORT COEFFICIENTS FOR WORMLIKE MICELLAR SOLUTIONS

Results are presented in this section for the macrotransport coefficients arising in situations for which the aggregation processes are represented by Eq. (B1). Derivation of the required size-space diffusion equation is effected in Appendix B, wherein we identify the size-space transport coefficients in Eqs. (B8) and (B16). Interesting features of this example, which contrast with the preceding spherical micellar case are (i) dependence of the mean aggregation number on micellar concentration; and (ii) the unique form of the potential energy function governing the size distribution. As in the spherical micellar example, the force $F(n)$ scales with n. The mobility coefficient $M(n)$, however, requires a bit more explanation. This example is analyzed in the spirit of extreme simplicity, omitting complications that necessarily accompany more realistic descriptions of polymer solution behavior, especially with regard to excluded-volume issues and the like [26]. Complications accompanying a more rigorous analysis can easily be accommodated within the general framework outlined in Sec. II.

Since our primary aim is to illustrate macroscopic effects resulting from fluctuations in the cluster aggregation number, rather than concentrating on detailed theories of polymer behavior in solutions we instead consider a simplistic model for the mobility of a polymer cluster, namely, the classical Debye-Bueche porous sphere model [27]. Research on the dynamics of polymer solutions is often based upon the geometric representation of polymers as macromolecular chains possessing an enormous number of degrees of freedom, and subsequently employing simplified kinetic models such as ''bead-spring'' or ''bead-rod'' models as well as extensions thereof (cf. Bird *et al.* [28]). In these models, hydrodynamic interactions among beads are either completely neglected or simplistically accounted for via use of the equilibrium preaveraged Oseen-Burgers tensor. In contrast, the porous sphere model proposed by Debye-Bueche accounts for hydrodynamic interactions by considering the hindered flow of the solvent through a permeable sphere composed of a cluster of resisting beads. Felderhof and Deutch [29] studied the relationship between the Kirkwood-Risemann [30] and Debye-Bueche theories. They concluded that both theories possessed an equivalent microscopic status, differing only in the statistical assumptions underlying their derivation. Further details regarding both motivation for and use of the porous sphere model can be found in Frankel, Mancini, and Brenner [11], wherein a related example involving size fluctuations of a porous-sphere, polymer model was studied. The essential scenario studied therein is similar in spirit to the case analyzed here, except that there the size fluctuations resulted from the inherently flexible nature of the polymer molecule undergoing thermal fluctuations, rather than from the A-D mechanism as outlined here.

According to the Debye-Bueche theory, the mobility coefficient of a uniformly homogeneous porous sphere of radius r and permeability K' moving through a solvent of viscosity μ is

$$M(r)=\frac{1}{6\pi\mu r}\left[\frac{1+(\frac{3}{2})K(1-K^{1/2}\tanh K^{-1/2})}{1-K^{1/2}\tanh K^{-1/2}}\right], \quad (42)$$

where $K=K'/r^2$ is the dimensionless Darcy permeability. The dimensional permeability is known [31] to scale inversely with the volume fraction of the chains (i.e., beads) comprising the porous sphere. In conjunction with the fact that the radius of the sphere scales with $n^{1/2}$, for an ideal random walk we obtain

$$K=\lambda n^{-1/2}, \quad (43)$$

where λ is a nondimensional proportionality constant. Using representative parametric values provided in Debye-Bueche's article the constant λ was estimated to be $O(1)$, whereupon we adopt the value $\lambda=5$ in this analysis. Substitution of Eq. (43) into Eq. (42) yields the requisite expression for $M(n)$.

The essential framework of the subsequent theory is similar to that illustrated in the preceding section. Accordingly,

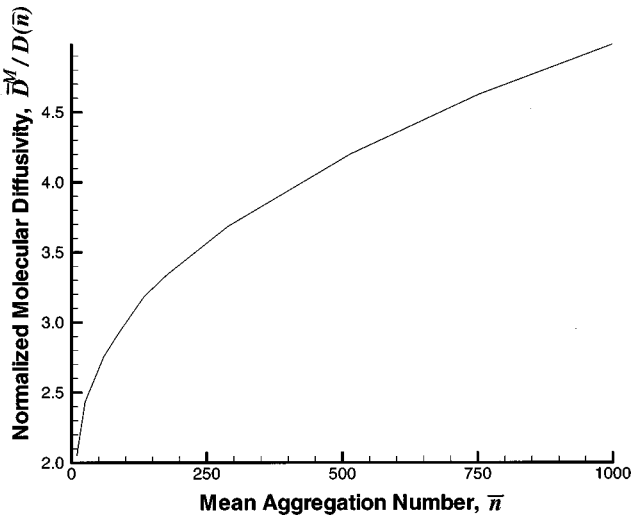

FIG. 7. Effect of mean aggregation number $\overline{n}$ on the normalized molecular diffusivity $\overline{D}^M/D(\overline{n})$ for wormlike micellar solutions.

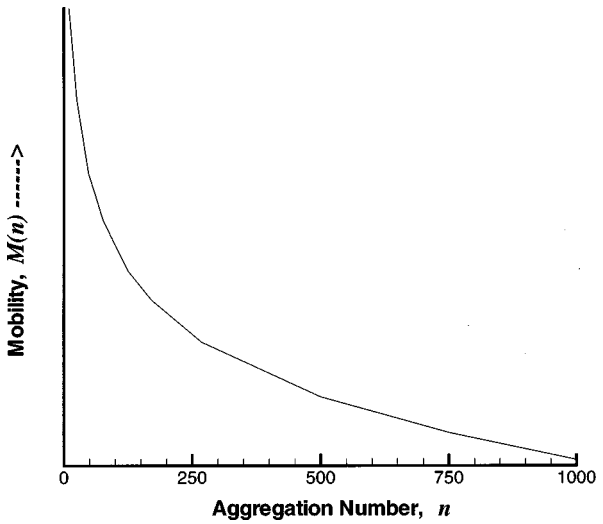

FIG. 8. Variation of the mobility $M(n)$ with size n for monodisperse wormlike micellar solutions. Since only qualitative features of this behavior are of interest we do not explicitly display values for $M(n)$ (a dimensional quantity).

we restrict ourselves in what follows only to the unique features of the wormlike micelle case, followed by a brief discussion of the results obtained. One of the features distinguishing the present case from the previous one is the concentration dependence of the mean micelle length. While this feature makes the present case more interesting, it simultaneously imposes certain constraints upon the mean aggregation number owing to our prior assumption of diluteness. Large mean aggregation numbers would necessarily imply high concentrations, nullifying the assumption of a dilute system. And at these high concentrations one encounters regimes wherein concentration effects arising from entanglement and reptation of polymer chains acquire heightened significance. Bouchaud and co-workers [17,18] have observed several interesting features accompanying diffusion in these regimes, including evidence for Levy flights (in contrast to the normal Brownian random walk). These effects, though interesting, are beyond the scope of the present work. We thus proceed with this caveat of limitations imposed by the diluteness criterion.

Using Eq. (B16), $P_0^\infty(n)$ can be obtained from Eq. (20) as

$$P_0^\infty(n)=\left[\int_1^\infty dn\,\exp(-n/\overline{n})\right]^{-1}\exp(-n/\overline{n}). \qquad (44)$$

This expression indicates that at a given value of n, $P_0^\infty(n)$ is functionally dependent only upon the mean aggregation number $\overline{n}$. In a manner similar to the scaling *ansatz* made in the previous section, all the macrotransport coefficients can be expected to scale as $f(\overline{n})$, with $f(x)\to x^\alpha$ for $x\gg 1$. Results obtained for the mean settling velocity, mean molecular diffusivity, and convective dispersivity are discussed below.

Mean velocity of settling. Figure 5 indicates the effect of cluster polydispersivity on the mean settling velocity $\overline{U}$. This mean settling velocity is almost identical to the settling velocity $U(\overline{n})$ at the mean aggregation number. The source of this behavior can be comprehended by analyzing the variation of the size-specific settling velocity $U(n)$ with aggregation number n. Figure 6 qualitatively depicts the settling velocity for different aggregation numbers. Due to a combination of effects resulting from the dependence of the force and mobility upon the aggregation number, this velocity increases with increasing aggregation number. On the other hand, the probability distribution (44) for the cluster size indicates an exponential decrease with aggregation number. Thus, larger velocities are sampled only infrequently and vice versa. Together, these factors nullify one another, resulting in an almost imperceptible effect of size distribution upon mean settling velocity.

Mean diffusivity of settling. Figure 7 depicts the effect of aggregation number on the mean molecular diffusivity. In contrast to the comparable settling velocity case, size effects here are quite significant. Mean diffusivity values at different aggregation numbers (in regimes which are expected to be classified as dilute) are seen to be greater by a factor of almost 2 to 3 than those arising at the mean aggregation number. The underlying reason for such behavior resides in the preferential sampling of the low aggregation number clusters, which in turn possess larger mobilities (Fig. 8). At high aggregation numbers the mean diffusivity appears to reach an asymptotic limit characteristic of the fact that the mobility and probability distribution both fall to zero at large n. However, at such large aggregation numbers the transport coefficients will depend primarily upon entanglement effects, in which circumstances the assumption of a dilute solution would clearly be invalid.

Convective dispersivity. Figure 9 displays the functional dependence of the convective dispersivity upon the mean aggregation number. Such size effects can be expected to be much more dramatic for the convective dispersivity case than for the other two macrotransport coefficients. As already noted, the convective dispersivity arises solely in response to the distribution of micelle sizes. An increase in mean aggregation number leads to a wider spread in the size distribution, exemplifying the exponential distribution (44) of sizes. Such behavior is consistent with the observed increase in convective dispersivity with increasing mean aggregation number. Based upon the dispersivity values ob-

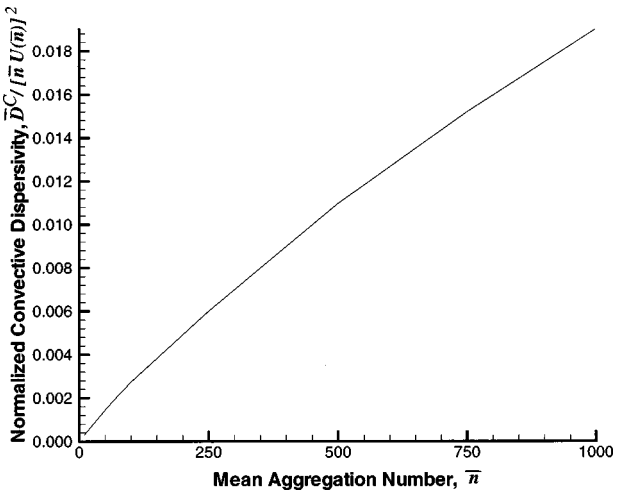

FIG. 9. Dependence of the normalized convective dispersivity $\overline{D}^C/[\overline{n}U(\overline{n})]^2$ on mean aggregation number $\overline{n}$ for wormlike micellar solutions.

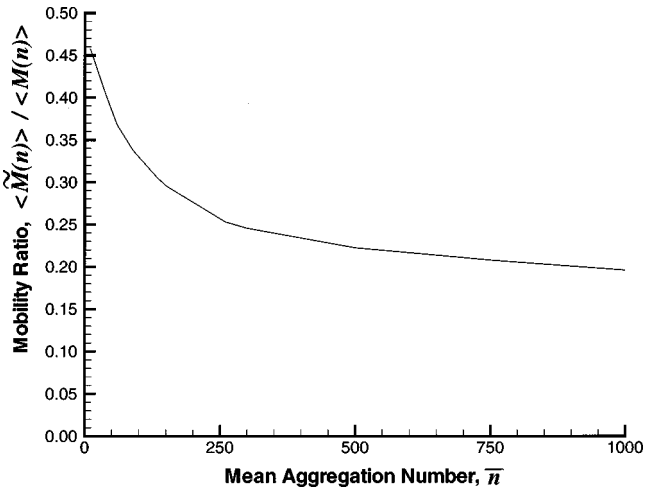

FIG. 10. Dependence of the mobility ratio $\langle\tilde{M}(n)\rangle/\langle M(n)\rangle$ on mean aggregation number $\overline{n}$ for wormlike micellar solutions.

served at large aggregation numbers the scaling exponent α for $\overline{D}^C/[\overline{n}U(\overline{n})]^2$ is empirically established to be about $\alpha \approx 0.7$.

Mean mobility. As in the spherical micelle case a mean mobility based on mean settling velocity can be defined [cf. Eq. (40)]. The variation in the resulting ratio of apparent-to-actual mean mobility is indicated in Fig. 10, again quantifying the apparent violation of the Stokes-Einstein relation.

Significance of results. The preceding discussion deals with size distribution effects on the macrotransport coefficients $\overline{U}$, $\overline{D}^M$, and $\overline{D}^C$ characterizing the transport of polydisperse wormlike micelles through the solution. Such polydispersivity effects appear to be specially pronounced for the mean molecular diffusivity case. Moreover, the presence of a Taylor dispersion contribution stems entirely from the polydispersivity of the micellar system. An order-of-magnitude estimate for this additional diffusivity contribution serves to quantify its significance in relation to the mean molecular diffusivity. From Fig. 9 we extract a ''typical'' value of $\overline{D}^C/[\overline{n}U(\overline{n})]^2 = 1000$. Consequently,

$$\frac{\overline{D}^C}{\overline{D}^M} \sim 10^{-3}\overline{n}^3 \frac{U(\overline{n})^2}{k_B T M(\overline{n})}. \tag{45}$$

Using approximate scaling relationships, namely, $U(\overline{n}) \sim n^{1/2}$ and $M(\overline{n}) \sim n^{-1/2}$ (not rigorously true for the porous sphere model) together with characteristic values of $M(\overline{n})$ to obtain the prefactor, we find that

$$\frac{\overline{D}^C}{\overline{D}^M} \sim 10^{-28}\overline{n}^{4.5} g^2, \tag{46}$$

with g denoting the dimensionless force. This suggests that the extra contribution to the diffusivity becomes significant only for very long macromolecules subject to large accelerations (such as would arise during ultracentrifugation). Despite the relatively small value predicted for the convective dispersivity under normal sedimentation conditions, we have shown that the effect of polydispersivity on the molecular diffusivity is a nontrivial one, leading to an increase in cluster mobility by a factor of almost 3. Furthermore, we have evaluated the functional dependence of the macrotransport coefficients on the mean aggregation number $\overline{n}$. In view of the relationship that exists between $\overline{n}$ and micellar concentration the above result can, *inter alia*, be considered as representing the effect of concentration on the transport coefficients. It is interesting to note that such an effect arises even in the dilute solution regime.

V. CONCLUSIONS

The preceding analysis furnishes a general framework for analyzing diffusion and sedimentation phenomena in systems exhibiting a distribution of cluster sizes stemming from the existence of reversible association-dissociation processes. Examples of such systems include micellar solutions and microemulsions. The generic scheme developed describes the transport of dilute dispersions of clusters through an otherwise quiescent solvent via the use of coarse-grained, size-independent, physical-space transport coefficients appearing in a convective-diffusion equation governing the local spatial cluster concentration (probability density). This was achieved through use of generalized Taylor dispersion theory.

Our scheme was illustrated by analyzing two practically motivated examples encountered in dealing with micellar solutions. In the first case we studied the aforementioned effects for a solution composed of spherical micelles. In such a scenario the cluster size is characterized by a Gaussian distribution about a mean aggregation number. Using known information about such solutions we quantified the mean transport coefficients in terms of typical micellar data available in literature. In the second case, similar effects were studied for cylindrical or wormlike micelles. Due to the reversible scission processes present in these latter systems they are widely regarded as models of ''living polymers.'' Interesting features arising for this case include an exponential attenuation of the size distribution with mean aggrega-

tion length. Furthermore, in such systems the mean aggregation length depends upon the micellar concentration. Thus, for this class of systems the macrotransport coefficients obtained in our work serve to quantify the variation of the transport coefficients with micellar concentration, at least in dilute systems.

A number of potential applications arise from the above results. Self-diffusion coefficients are often employed to provide a measure of mean aggregation numbers in spherical micellar solutions, at least in circumstances where such solutions may be regarded as being approximately monodisperse. Our analysis provides a scheme whereby polydispersivity effects can be incorporated into the interpretation of experimental results so as to furnish estimates of the errors arising from a lack of true monodispersivity. Moreover, our analysis is sufficiently general to also embrace the effects of micellar shape (such differences being embodied in the constitutive forms assumed for the microscale potential and the mobility coefficients) on the macroscale transport coefficients. This constitutes a possible future application for determining the mean properties of such micelles in solution from measurements of their settling (or electrophoretic) velocities and mean self-diffusivities [8]. Furthermore, the fact that our generic analysis is not restricted exclusively to micellar applications permits possible extensions towards studying the effects of ''mixing'' on the kinetics of aggregation processes. Such an investigation would involve the opposite extreme of time scales, whereby the A-D kinetic time scale is more sluggish than the physical-space transport time scales. Our analysis points up a scheme whereby a systematic study of these effects could be pursued.

ACKNOWLEDGMENTS

This work was supported jointly by both the Office of Basic Energy Sciences and the Mathematical, Information, and Computational Sciences Division of the U.S. Department of Energy. Useful discussions with Vibha Srinivasan, Daniel Kamei, and Professor Shimon Haber are acknowledged.

APPENDIX A: SIZE-SPACE DIFFUSION EQUATION DESCRIBING STEPWISE ASSOCIATION

1. Basic reaction

Step-wise association schemes serve as models of the association-dissociation (A-D) processes governing the growth of spherical micelles [32]. Herein, the basic unit is taken to be a monomer, denoted by A_1. The A-D scheme can then be portrayed as a reversible reaction of the following general form:

$$A_{n-1}+A_1 \underset{k_{n-1}^-}{\overset{k_{n-1}^+}{\rightleftharpoons}} A_n, \tag{A1}$$

wherein A_n denotes a cluster containing n monomers. The micellar solution is assumed to be at equilibrium (sizewise) at the start of the observation process. We then select a monomer molecule bound to a cluster as our tracer and subsequently follow its evolution as it moves through the solvent. This monomer tracer can undergo the following transport processes: (i) diffusion and sedimentation bound to a cluster of the same size; (ii) transport bound to a cluster of a different size resulting from A-D processes of monomers to and from the original cluster; (iii) dissociation of the tracer monomer from the cluster to recombine with another cluster. During each of these processes the tracer undergoes physical-space transport representative of a cluster the dimensions of which are identical to that of the cluster to which the monomer is instantaneously attached. As such, the monomer tracer undergoing these transport processes may be equivalently represented by a tracer cluster undergoing continuous changes in size, simultaneous with the cluster undergoing movement through the fluid continuum. In the following, a tracer cluster will be taken to denote a cluster with $n>2$. As elucidated later, transport by mechanism (iii), which occurs when the tracer is present as a monomer, is accounted for in an indirect manner.

The procedure employed to derive the size-space diffusion equation is outlined below. This scheme is identical to that employed in the next section to derive the comparable equation for the case of a wormlike micelle. In either case we consider a solution initially at equilibrium with respect to transport in size space (i.e., one wherein the equilibrium size distribution prevails). Into this solution we imagine a tracer cluster to be added, which then undergoes physical-space transport as well as the reversible A-D processes described by Eq. (A1). As is rigorously proved within the framework of generalized Taylor dispersion theory, the initial size of such a cluster proves irrelevant in the calculation of macrotransport coefficients. In addition to the original assumption of an equilibrium solution (requiring that the concentration of ''nontracer'' clusters satisfy the law of mass action [34]) we subsequently employ a master equation approach to quantify the rate of change of the cluster probability distribution, thereby obtaining an appropriate continuous size-space transport equation governing movement of the tracer cluster.

2. Master equation for the tracer

Based on the above reaction scheme for representing the A-D processes one can write a master equation for $P(n)$ (the explicit time dependence of which is notationally suppressed), namely, the probability that the tracer is present in a cluster containing n monomers, including itself, irrespective of its position in the physical space. Such an equation is derived by considering the possible A-D reactions undergone by the *tracer* cluster containing n monomers (denoted as A_n^*):

$$A_{n-1}^*+A_1 \underset{k_{n-1}^-}{\overset{k_{n-1}^+}{\rightleftharpoons}} A_n^*, \tag{A2}$$

$$A_n^*+A_1 \underset{k_n^-}{\overset{k_n^+}{\rightleftharpoons}} A_{n+1}^*. \tag{A3}$$

Accordingly, the master equation governing the probability $P(n)$ satisfies the equation

$$\frac{dP(n)}{dt}=k_{n-1}^{+}P(n-1)X_1-k_{n-1}^{-}P(n)+k_n^{-}P(n+1)-k_n^{+}P(n)X_1, \tag{A4}$$

in which X_1 denotes the concentration of the free monomeric species. As a simplification we assume that k^- is independent of n. This will subsequently be shown to be equivalent to the assumption that $d(n)$ in (5) is independent of n. While the prescription in Sec. II is general enough to treat other cases, we nevertheless invoke this assumption so as to focus exclusively upon the effect of the A-D processes on the physical-space macrotransport coefficients. Based on the above assumption we obtain

$$\frac{dP(n)}{dt}=k^-\left[\frac{k_{n-1}^{+}}{k^-}P(n-1)X_1-P(n)+P(n+1)-\frac{k_n^{+}}{k^-}P(n)X_1\right]. \tag{A5}$$

Equilibrium considerations for reactions (A2) and (A3) on the other hand require that

$$\frac{k_{n-1}^{+}}{k^-}=\exp\left[-\frac{(\mu_n^*-\mu_{n-1}^*-\mu_1^0)}{k_BT}\right],\qquad \frac{k_n^{+}}{k^-}=\exp\left[-\frac{(\mu_{n+1}^*-\mu_n^*-\mu_1^0)}{k_BT}\right], \tag{A6}$$

in which μ_n^* denotes the standard-state chemical potential of the cluster of size n. The latter is equal to the free energy change occurring when a cluster of size n is introduced into the pure solvent; μ_1^0 represents the comparable standard-state chemical potential of the monomer [33]. For the dilute solutions assumed, the chemical potential μ_1 of the monomer can be expected to obey the ideal solution relation

$$\mu_1=\mu_1^0+k_BT\ln X_1. \tag{A7}$$

Upon using Eq. (A7) and writing $\mu_1^0=n\mu_1^0-(n-1)\mu_1^0$ we obtain

$$\frac{k_{n-1}^{+}X_1}{k^-}=\exp\left\{-\frac{[\mu(n)-\mu(n-1)]}{k_BT}\right\},\qquad \frac{k_n^{+}X_1}{k^-}=\exp\left\{-\frac{[\mu(n+1)-\mu(n)]}{k_BT}\right\}. \tag{A8}$$

In the above, $\mu(n)\equiv\mu_n^*-n\mu_1$. Insertion of the above identification into Eq. (A5) yields

$$\frac{dP(n)}{dt}=k^-\left\{P(n-1)\exp\left[-\frac{[\mu(n)-\mu(n-1)]}{k_BT}\right]-P(n)+P(n+1)-P(n)\exp\left[-\frac{[\mu(n+1)-\mu(n)]}{k_BT}\right]\right\}. \tag{A9}$$

van Kampen's [35] expansion method may be utilized in the above discrete master equation to derive the aggregation-space diffusion equation corresponding to the limit of a continuous variation of sizes. This continuum limit is obtained by introducing a parameter Ω denoting the density of the discrete variable n, followed by an expansion in $1/\Omega$. Upon setting $x=n/\Omega$, $P(x\Omega)=p(x)$ and $\mu(x\Omega)/k_BT=v(x)$, Eq. (A9) becomes

$$\frac{dp(x)}{dt}=k^-\left[p\left(x-\frac{1}{\Omega}\right)\exp\{-[v(x)-v(x-1/\Omega)]\}-p(x)+p\left(x+\frac{1}{\Omega}\right)-p(x)\exp\{-[v(x+1/\Omega)-v(x)]\}\right]. \tag{A10}$$

The right-hand side of the above equation can be expanded in a Taylor series in x and the resultant expression simplified. For the sake of brevity the details of such an exercise are omitted here, the ultimate result being

$$\frac{\partial p(x)}{\partial t}=\frac{k^-}{\Omega^2}\frac{\partial}{\partial x}\left[\frac{\partial p}{\partial x}+p(x)\frac{\partial v}{\partial x}\right]+O\left(\frac{1}{\Omega^4}\right). \tag{A11}$$

To terms of leading order, the above equation resembles a diffusion equation in the presence of a field of force, which can be recast in terms of our original variables as

$$\frac{\partial P(n)}{\partial t}=k^-\frac{\partial}{\partial n}\left\{\frac{\partial P}{\partial n}+P(n)\frac{\partial[\mu(n)/k_BT]}{\partial n}\right\}. \tag{A12}$$

The latter is equivalent to the diffusion equation

$$\frac{\partial P(n)}{\partial t}+\frac{\partial j}{\partial n}=0 \tag{A13}$$

[cf. Eqs. (3) and (7)], wherein the following identifications hold [in Eq. (5)]:

$$m(n)=k^-,\quad V(n)=\mu(n),\quad d(n)=k^-. \tag{A14}$$

The relationship between Eqs. (A13) and (3) is such that the former may be regarded as a transport equation in size space for circumstances where the ''source term'' $\nabla\cdot J=0$, such as would be the case when the probability density P appearing in Eqs. (3)–(7) was independent of $\mathbf{R}$.

3. Model for μ_n^0

This section deals with the identification of the potential $V(n)\equiv\mu(n)$. Experimental observations [33] in spherical micellar solutions indicate the existence of an equilibrium size distribution characterized by a slight degree of polydispersivity centered around a mean aggregation number. Based on these observations we use the following simple quadratic model for the potential:

$$\frac{V(n)}{k_BT}=\hat{V}_0+\frac{(n-\bar{n})^2}{2\sigma^2}, \tag{A15}$$

where $\bar{n}$ represents the mean aggregation number and σ quantifies the degree of polydispersivity. The numerical value of constant $\hat{V}_0=V(\bar{n})/k_BT$ proves to be irrelevant under subsequent normalization. Furthermore, in the ensuing

analysis k^- will be set to unity without any loss of generality. This completes the size-space identifications prerequisite to performing explicit calculations of the macrotransport coefficients.

4. Time scales

Our coarse-grained quantification of the overall transport process can be justified only in circumstances for which the time scales T characterizing the A-D processes are much less than those characterizing the physical-space transport processes, thereby enabling us to assume an instantaneous size-space equilibrium distribution despite a comparable lack of equilibrium in physical space. Typical values describing the kinetics of the aggregation process involve time scales of microseconds to milliseconds [1,32]. On the other hand, transport in physical space typically involves a diffusion coefficient of $O(10^{-5}\,\mathrm{cm}^2/\mathrm{s})$ [7]. For a dilute solution (wherein the mean interparticle separation is quite large) one can easily corroborate the assertion that $T(\text{physical-space diffusion}) \gg T(\text{kinetics})$.

5. Transport by mechanism (iii)

In the above analysis the cluster has been consistently assumed to be of a size such that $n>2$, with the possibility of transport as a monomer ignored. The reason for such an approach resides in the fact that a monomer does not satisfy the general form of the master equation (A4). Under the long-time limit considered in Sec. III, the tracer can be expected to possess a probability $X_1/X_s \equiv p$ of evolving as a monomer, where X_s is the total solute concentration in the solution. Thereby, the normalization condition (19) needs to be modified to the form

$$\int_1^\infty dn\, P_0^\infty = 1-p. \tag{A16}$$

However, we ignore the above constraint with the understanding that the macrotransport coefficients $\overline{U}$, $\overline{D}$, etc., as calculated in Sec. III, need to be corrected for the presence of monomer transport by appropriate renormalization, e.g.,

$$\overline{M}\ \ (\text{Sec. IV}) = \frac{\overline{M}\ \ (\text{actual})}{1-p} - \frac{pM\ \ (\text{monomer})}{1-p}, \quad \text{etc.} \tag{A17}$$

APPENDIX B: SIZE-SPACE DIFFUSION EQUATION FOR A WORMLIKE MICELLE (LIVING POLYMER)

Wormlike micelles provide an interesting class of micellar entities, distinct from the spherical micelles considered in the previous section. Studies of these systems were pioneered by Cates [15,16]. Unlike spherical micellar solutions, which display an equilibrium size distribution peaked around a mean aggregation number $\overline{n}$, wormlike micelles manifest a range of sizes extending over a significant interval. The latter scenario provides a natural background to illustrate extremal size-distribution effects. Explicitly, this section is concerned with the derivation of the size-space diffusion equation for a tracer cluster (the labeling of which is carried out in a manner similar to that of the previous section). Since a number of details are similar to those of the preceding section, only essential distinguishing features are outlined here.

1. Basic reaction

In contrast to the stepwise association scheme of the preceding case, we here assume scission, recombination, and growth from micelles of arbitrary sizes. The reaction step is represented by the equation

$$A_n + A_{n'} \underset{k^-(n+n')}{\overset{k^+(n;n')}{\rightleftharpoons}} A_{n+n'}. \tag{B1}$$

As in the previous section we consider a solution which is originally at equilibrium (in size space) wherein we effect the tracer observation. Furthermore, as in the preceding example, $k^-(n)$ is assumed to be independent of n.

2. Master equation for the tracer

The above reaction scheme for characterizing the A-D process enables us to write a master equation for $P(n)$, the probability that the tracer is present in a cluster containing n monomers (including itself). The reaction pathways undergone by the tracer cluster are represented by the scheme

$$A_n^* + A_{n'} \underset{k^-}{\overset{k^+(n;n')}{\rightleftharpoons}} A_{n+n'}^*, \tag{B2}$$

$$A_{n-n'}^* + A_{n'} \underset{k^-}{\overset{k^+(n-n';n')}{\rightleftharpoons}} A_n^*. \tag{B3}$$

The above reaction sequence yields

$$\frac{dP(n)}{dt} = \int dn' [k^- P(n+n') - k^+(n;n')P(n)C(n') + k^+(n-n';n')P(n-n')C(n') - k^- P(n)], \tag{B4}$$

wherein $C(n)$ represents the concentration of clusters of size n in the solution. Equilibrium considerations, however, require that

$$\frac{k^+(n;n')}{k^-} = \exp\left[-\frac{(\mu_{n+n'}^* - \mu_n^* - \mu_{n'}^0)}{k_B T}\right];$$

$$\frac{k^+(n-n';n')}{k^-} = \exp\left[-\frac{(\mu_n^* - \mu_{n-n'}^* - \mu_{n'}^0)}{k_B T}\right], \tag{B5}$$

where the symbols μ_n^*, etc. possess the same meanings as in Appendix A. Furthermore, since the original solution was assumed to be at equilibrium in size space, the chemical potentials of clusters of sizes n, n' and $n+n'$ (denoted, respectively, as $\mu_n, \mu_{n'}$ and $\mu_{n+n'}$) satisfy the equilibrium condition corresponding to the reaction (B1), viz.,

$$\mu_{n'} + \mu_n = \mu_{n+n'}, \tag{B6}$$

where the μ_n's are assumed to obey an ideal solution law of the form

$$\mu_n = \mu_n^0 + k_B T \ln C(n). \tag{B7}$$

Based upon the above considerations it is straightforward to implement an expansion of the above master equation, as was done in the preceding section. The resulting equation is of the same form as follows from Eq. (A4) [cf. remarks following Eq. (A14) for the correspondence to Eq. (3)], wherein the following identifications hold:

$$m(n) = k^-; \quad V(n) = \mu(n) \equiv \mu_n^* - \mu_n^0 \equiv k_B T \ln C(n);$$

$$d(n) = k^-. \tag{B8}$$

In addition to a different size distribution from the spherical micellar case we observe another interesting feature of this model, namely, the dependence of $V(n)$ upon the micellar concentration of the solution through $C(n)$. It is pertinent to observe that the solution is nevertheless still considered to be a dilute, ideal solution, in which hydrodynamic and intercluster physicochemical interactions are both completely neglected. The manifestation of the A-D processes through the concentration dependence of the macrotransport coefficients provides an interesting, unconventional source of nonideality.

3. Equilibrium

Calculation of the transport coefficients necessitates obtaining the equilibrium concentration distribution in the micellar solution. Upon invoking the equilibrium condition for Eq. (B1) we find that

$$\frac{k^+(n;n')}{k^-} = \frac{C(n+n')}{C(n)C(n')} = \exp\left\{ - \frac{[\mu_{n+n'}^0 - \mu_n^0 - \mu_{n'}^0]}{k_B T} \right\}. \tag{B9}$$

Based on the latter we make the following ansatz for the equilibrium concentration (cf. also Cates [15]):

$$C(n) = \exp(-\mu_n^0 - \alpha n), \tag{B10}$$

where α is a constant to be determined via the normalization condition imposed upon the concentration. Additionally, μ_n^0 represents the standard chemical potential of a cluster consisting of n monomers.

For wormlike micelles, which are inherently two dimensional, it is conventional to assume a standard chemical potential of the form [33]

$$\frac{\mu_n^0}{n} = \hat{\mu}_\infty^0 + \frac{A}{n}, \tag{B11}$$

where A is a constant reflecting the energetic interactions occurring within the cluster, and

$$\hat{\mu}_\infty^0 \overset{\text{def.}}{=} \lim_{n\to\infty} \frac{\mu_n^0}{n}.$$

This prescription for the standard chemical potential μ_n^0 retains the form of the ansatz proposed for the equilibrium concentration $C(n)$, wherein the constant α is replaced by another constant, namely, $\alpha' \equiv \alpha + \hat{\mu}_\infty^0$. Consequently,

$$C(n) = \beta \exp(-\alpha' n), \tag{B12}$$

with β a constant that can be determined from the specified microscale parameters. Use of the normalization condition for the total solute concentration C, namely,

$$\int_0^\infty dn\, nC(n) = C, \tag{B13}$$

yields

$$\frac{\beta}{(\alpha')^2} = C. \tag{B14}$$

If we define a mean aggregation number $\bar{n}$ as

$$\frac{\int_0^\infty dn\, nC(n)}{\int_0^\infty dn\, C(n)} = \bar{n}, \tag{B15}$$

then, using Eqs. (B8) and (B10)–(B15), we obtain

$$V(n) = -\frac{n}{\bar{n}} + V_0, \tag{B16}$$

with $V_0 \equiv V(0)$ an arbitrary constant which will prove irrelevant under normalization of the probability.

This completes our identification of the potential $V(n)$ in terms of the aggregation number n. This potential is dependent upon the single parameter $\bar{n}$, the latter representing the mean aggregation number. In contrast with the spherical micellar solution case, this mean aggregation number can be shown [33] to be proportional to $\sqrt{C}$ [using Eqs. (B14) and (B15)]. As such, investigating the effect of the parameter $\bar{n}$ on the transport coefficients is equivalent to investigating the comparable effect of micellar concentration. As already noted, this concentration effect on the transport coefficients, even in the dilute limit considered, constitutes an interesting phenomena with origins in the clustering phenomena taking place within these systems.

4. Time scales

As in the preceding section we need to justify *a posteriori* the legitimacy of the coarse-graining process in terms of the time scales involved. Typical values of the kinetic time scales arising in these systems are quoted by Ott *et al.* [18], wherein the time scale of recombination and scission was estimated to be of the order of 100 ms. In contrast, the time scales characterizing physical-space diffusion of these especially large molecules through dilute systems, such as here envisioned, can be expected to be of the order of hours. This justifies our assumption that the size-space diffusional process can be ''projected out,'' resulting in a coarse-grained three-dimensional diffusion process that accurately portrays the overall transport phenomena in physical space without invoking the classical preaveraging assumption.

[1] R. J. Hunter, *Foundations of Colloid Science* (Oxford University Press, New York, 1987).
[2] B. Lindman and P. Stilbs, in *Microemulsions: Structure and Dynamics*, edited by S. E. Friberg and P. Bothorel (CRC, Boca Raton, FL, 1987).
[3] W. M. Gelbart, A. Ben-Shaoul, and D. Roux, *Micelles, Membranes, Microemulsions and Monolayers* (Springer-Verlag, Berlin, 1994).
[4] J. Israelachvili, *Intermolecular & Surface Forces* (Academic, New York, 1991).
[5] P. Hebraud and F. Lequeux, e-print cond-mat/9805373.
[6] P. Sollich, F. Lequeux, P. Hebraud, and M. E. Cates, Phys. Rev. Lett. **78**, 2020 (1996).
[7] D. Chatenay, W. Urbach, R. Messager, and D. Langevin, J. Chem. Phys. **86**, 2343 (1987).
[8] D. Chatenay, W. Urbach, M. Cazabat, and D. Langevin, Phys. Rev. Lett. **54**, 2253 (1985).
[9] W. Urbach, H. Hervet, and F. Rondelez, J. Chem. Phys. **83**, 1877 (1985).
[10] E. L. Cussler, AIChE. J. **26**, 43 (1980).
[11] I. Frankel, F. Mancini, and H. Brenner, J. Chem. Phys. **95**, 8636 (1991).
[12] A. Ziabicki, J. Chem. Phys. **85**, 3042 (1986).
[13] C. Angelious, M. Psimopoulos, and G. J. Jameson, Chem. Eng. Sci. **34**, 671 (1979).
[14] H. Brenner and D. A. Edwards, *Macrotransport Processes* (Butterworth-Heinemann, Newton, MA, 1993).
[15] M. E. Cates, Macromolecules **20**, 2289 (1987).
[16] M. E. Cates, J. Phys. (France) **49**, 1593 (1988).
[17] J. P. Bouchaud, A. Ott, D. Langevin, and W. Urbach, J. Phys. II **1**, 1465 (1991).
[18] A. Ott, J. P. Bouchaud, W. Urbach, and D. Langevin, J. Phys. II **7**, 1099 (1997).
[19] Because the physical space is assumed infinite and homogeneous throughout, only the difference $\mathbf{R}-\mathbf{R}'$ appears, rather than $\mathbf{R}$ and $\mathbf{R}'$ separately.
[20] A. Einstein, *Theory of Brownian Motion* (Dover, New York, 1956).
[21] I. Frankel and H. Brenner, J. Fluid Mech. **204**, 97 (1989).
[22] The exponent ν can be obtained from the knowledge of the variation of ψ with $\overline{n}$ for a monodisperse solution.
[23] I. S. Gradshteyn and I. M. Ryzhik, *Table of Integrals, Series and Products* (Academic, New York, 1980).
[24] Denote $n/\overline{n}=x$. Then the average of weights of two sizes $n-\overline{n}$ and $n+\overline{n}$ on either side of the mean aggregation number is $\propto\frac{1}{2}[(1-x)^{2/3}+(1+x)^{2/3}]\propto(1-\frac{1}{9}x^2)<1$.
[25] Since $n^{2/3}\to 0$ as $n\to 0$, for large $\tilde{\sigma}$ the expression for the mean velocity can be written approximately in this limit as $\int_0^\infty dn\, n^{2/3}\exp(-n^2/2\tilde{\sigma}^2)/\int_0^\infty dn\,\exp(-n^2/2\tilde{\sigma}^2)\sim\tilde{\sigma}^{2/3}$ by simple scaling arguments.
[26] H. Yamakawa, *Modern Theory of Polymer Solutions* (Harper & Row, New York, 1971).
[27] P. Debye and A. M. Bueche, J. Chem. Phys. **16**, 573 (1948).
[28] R. B. Bird, C. F. Curtiss, R. C. Armstrong, and O. Hassager, *Dynamics of Polymeric Liquids* (Wiley-Interscience, New York, 1987).
[29] B. U. Felderhof and J. M. Deutch, J. Chem. Phys. **62**, 2391 (1975).
[30] J. G. Kirkwood and J. Riseman, J. Chem. Phys. **16**, 565 (1948).
[31] F. W. Wiegel, *Fluid Flow Through Porous Macromolecular Systems* (Springer, New York, 1980).
[32] E. A. G. Aniansson and S. N. Wall, J. Phys. Chem **78**, 1024 (1974).
[33] J. Israelachavili, D. J. Mitchell, and B. W. Ninham, J. Chem. Soc., Faraday Trans. 2 **72**, 1525 (1976).
[34] Note that the assumption of an initially equilibrium solution is not equivalent to the (incorrect) requirement that the size-space probability distribution of the tracer cluster possesses its equilibrium value. The introduction of a tracer cluster into a bath of clusters that are at equilibrium disturbs the bath only mildly; nevertheless it has a nontrivial effect on the unsteady-state development of the cluster size-space probability distribution.
[35] N. G. van Kampen, *Stochastic Processes in Physics and Chemistry* (North-Holland, Amsterdam, 1992).